International Journal of Heat and Mass Transfer 164 (2021) 120542

Contents lists available at ScienceDirect

International Journal of Heat and Mass Transfer

journal homepage: www.elsevier.com/locate/hmt

Theoretical analysis on droplet vaporization at elevated temperatures and pressures

Dehai Yu, Zheng Chen*

BIC-ESAT, SKLTCS, CAPT, Department of Mechanics and Engineering Science, College of Engineering, Peking University, Beijing 100871, China

ARTICLE INFO

Article history:
Received 9 July 2020
Revised 31 August 2020
Accepted 25 September 2020

Keywords:
Droplet vaporization
Heating time
Vaporization time
Surface temperature
Enthalpy of vaporization

ABSTRACT

Droplet vaporization has a great impact on combustion of liquid fuels and might greatly affects the engine performance. Physical understanding and theoretical interpretation of the droplet vaporization behavior are decisive to constitute appropriate models for spray combustion. In this work, we proposed a fully transient formulation for the droplet vaporization at wide ranges of temperature and pressure. The governing equations are solved analytically by means of suitable coordinate transformations. The droplet surface temperature and mass fraction of fuel vapor are determined by the matching conditions at the liquid-gas interface. Accordingly, a theoretical model, characterizing the time change of droplet size during its vaporization, is proposed in terms of the unsteadiness factor and droplet vaporization lifetime. The theoretical model successfully reveals the conventional recognition of droplet vaporization characteristics, and its predicted droplet size history agrees well with experimental results reported in the literature. Besides, based on the present theoretical analysis, the experimentally observed dual effect of pressure upon droplet vaporization is analyzed with help of an explicit formula for enthalpy of vaporization indicating its temperature-dependence.

1. Introduction

Liquid fuels are widely used in various engines, e.g., diesel engines, jet engines, and liquid rocket engines. To facilitate combustion, the injected fuel is atomized into exceedingly small droplets with diameters in micrometer scale [1–3]. In spray combustion system, the gasified fuel vapor participates combustion in gas phase, which releases a huge amount of heat and hence increases environmental temperature. The elevated temperature would facilitate the evaporation process of the droplets in the spray. It has been experimentally observed that only the larger droplets can penetrate the flame zone and burn individually, while the majority of the atomized droplets evaporates in the relatively cool interior of the spray [4]. Therefore, droplet vaporization plays a crucial role in engines and is of primary concern in a variety of multi-phase combustion studies.

Experimental studies on droplet vaporization under microgravity conditions without natural convection indicate that the vaporization lifetime decreases monotonically as ambient temperature increases [4,5]. Moreover, the droplet surface regresses more rapidly at elevated pressures [5,6]. In experiments, it is very difficult to generate an isolated droplet in stagnant environment without external support, and usually a single droplet is suspended by a thin fiber [5–7]. The suspension technique requires the droplet diameter to be considerably larger than the fiber thickness. Besides, the fiber attachment may cause droplet deformation, which becomes progressively severe with droplet size reducing.

In numerical simulations, different factors that affect droplet vaporization can be isolated and examined independently. Moreover, the evolutions of droplet temperature and diameter can be studied in simulations in wide ranges of pressure and temperature that resemble the engine operating conditions [8–21]. At elevated pressures, various fluid dynamic and thermodynamic non-idealities show profound impacts on the behavior of droplet vaporization [7,8,18,19]. The enthalpy of vaporization decays with the growth of droplet temperature, which results from the increment of ambient pressure [22]. The reduction of enthalpy of vaporization leads to increment of vaporization rate due to the increasing of Spalding transfer number as indicated in d^2-law [8,23]. Meanwhile, with the increase of pressure, the initial unsteady heating period increases and so does the droplet lifetime [11,15,16,24]. Such a dual effect of the ambient pressure is further affected by the ambient temperature. When the droplet reaches its thermodynamic critical state, the vanishing of liquid-gas interface, the enhanced solvability of environment gas in droplet fluid, and the anomalies in various thermal transport properties may lead to additional intricacy to the vaporization process [8,16,18].

* Corresponding author.
E-mail address: cz@pku.edu.cn (Z. Chen).

https://doi.org/10.1016/j.ijheatmasstransfer.2020.120542
0017-9310/

Nomenclature

a	coefficient in Peng-Robinson equation of state
b	coefficient in Peng-Robinson equation of state
c_p	heat capacity at constant pressure
c_v	heat capacity at constant volume
d	droplet diameter
D	mass diffusivity
d_0	initial droplet diameter
d_n	d/d_0
f_E	$R(T_c - T_R)/L_R$
k	Boltzmann constant
k_w	Watson characterization factor
L	enthalpy of vaporization
Le	Lewis number
$\dot{m}_F$	fuel vapor production rate
p	pressure
p_e	saturated vapor pressure
q_l	coordination number
r	radial coordinate
R	universal gas constant
r_s	droplet radius
s_g	specific gravity of n-heptane
t	time
T	temperature
$T_{b,\,n}$	boiling temperature at $p = 1$ atm
T_{ch}	$2T_s^0/3 + T_\infty/3$
t_L	$(T - T_R)/(T_c - T_R)$
t_n	t/t_{total}
T_s^0	droplet surface temperature during quasi-steady vaporization
T^*	$kT_{\mathrm{ch}}/\sqrt{\varepsilon_F \varepsilon_N}$
V_m	molar volume
W	molar mass
W_{FN}	$2(1/W_F + 1/W_N)^{-1}$
X	molar fraction
Y	mass fraction
Y_{Fs}^0	mass fraction of fuel vapor during quasi-steady vaporization

Greek symbols

α	critical exponent for heat capacity
β	critical exponent for density discrepancy
δ_w	width of transition region
ε	characteristic Lennard-Jones energy
λ	thermal conductivity
ξ	transformed radial coordinate
ρ	density
σ	non-dimensional radial coordinate
τ	non-dimensional time
Φ_i	$t_{\mathrm{heating}}/t_{\mathrm{total}}$
χ	characteristic Lennard-Jones length
ω	acentric factor
Ω_D	dimensionless collision integral

Subscripts

c	critical state
F	fuel species
g	gas phase
l	liquid phase
N	nitrogen
R	reference state in evaluating enthalpy of vaporization
s	quantities at droplet surface
∞	environmental condition at far field

In the simulation of spray combustion, simultaneous consideration of a huge number of droplets is a formidable task, which desires theoretical models for droplet vaporization [1,3,25]. The primary theory is the d^2-law, i.e., the square of droplet diameter decreases linearly with time, which is considered as the leading order solution for a variety of modified theories [19,26,27].

By assuming quasi-steady gas-phase process, Law and Sirignano [28–31] conducted a series of theoretical studies on unsteadiness of droplet vaporization and combustion with the emphasis on transient heating effects. They proposed and analyzed two models for droplet heating, i.e., distillation limit and conduction limit. The droplet surface regresses as the liquid fuel is converted into fuel vapor during vaporization. The moving boundary effect plays a crucial role in droplet vaporization problems and in the meanwhile causes mathematical difficulty in analytical solution of the governing equations for droplet vaporization. In a series of theoretical studies conducted by Law and Sirignano [29,32], the radial coordinate is scaled by the radius of the droplet, yielding a dimensionless spatial coordinate. Accordingly, the moving boundary is formally replaced by a fixed boundary where the non-dimension radial coordinate is equal to unity, and hence facilitates the analytical solution of the governing equations. Equivalent mathematical treatments were widely in theoretical studies upon droplet vaporization, considering the droplet vaporization lifetime at subcritical and supercritical conditions [13] as well as the influence of thermal expansion flow on droplet vaporization [33].

Assuming the density ratio between the gas and liquid, ρ_g/ρ_l, as a small parameter, Crespo and Linan [26] conducted asymptotic analysis for droplet vaporization in a stagnant atmosphere considering the unsteady effects in gas phase. They corrected the droplet lifetime by a factor of $\sqrt{\rho_g/\rho_l}$. Zugasti et al. [13] extended the preceding asymptotic analysis to supercritical conditions by discarding the liquid-gas interface and treating the droplet and ambient gas respectively as cold and hot fluid packages. They derived a transcendental equation, which interprets the evolution of the cold package radius and reproduces the d^2-law results for isothermal conditions in the cold region. Cossali and Tonini [34]. analyzed the droplet evaporation and solved the governing equations characterizing the steady-state mass, momentum and energy balance of vapor and gas mixture surrounding the droplet. Based on steady-state assumption, Cossali and Tonini [35] also proposed an analytical model of heat and mass transfer from liquid droplet, in which the thermo-physical properties of gas phase, e.g., density, heat capacity, diffusion coefficient, and thermal conductivity, were considered as functions of temperature. Snegirev [36] analyzed the vaporization of a single-component droplet with emphasis on the transient temperature gradient of the droplet. According to Snegirev, the droplet temperature was either approximated by mathematical models, e.g., parabolic, power-law, and polynomial functions of radial coordinate, or evaluated through heat balance integral method in terms of volume-averaged temperature [36]. Sazhin *et al.* [37–39] conducted a series of theoretical studies, considering the transient heating of a droplet immersed into a hot gas. According to their conclusions, the inhomogeneous gas temperature distribution may lead to slowing down of body heating, while the distribution of body temperature did not depend on the initial gas temperature inhomogeneity in the long-time limit.

Nevertheless, at elevated pressures, the prolonged droplet heating stage results in pronounced unsteadiness in the overall vaporization process. This prevents the direct utilization of d^2-law to interpret the droplet size history. Moreover, the density ratio, ρ_g/ρ_l, may not be treated as a small parameter at high pressures [40], which reduces the accuracy of the asymptotic analysis. To acquire insightful understanding of droplet vaporization and to accurately model the spray combustion, we need develop an accurate theoretical model which can quantitatively interpret the droplet vapor-

ization at wide ranges of temperature and pressure conditions. The model should explicitly reveal the impacts of various fluid dynamic and thermodynamic properties on the vaporization process. Therefore, it requires a comprehensive theoretical analysis, considering the transient effects and in the meanwhile appropriately dealing with the phase transition at the liquid-gas interface. Besides, it is recognized that the boiling temperature of a liquid increase with environmental pressure. Thereby, the droplet surface temperature would be higher at elevated ambient pressures, and so is the average temperature of the droplet. On the one hand, it leads to lengthening of droplet heating period, and on the other hand, lowers the enthalpy of vaporization and hence facilitates the vaporization rate. Thereby, the pressure plays a dual effect towards the droplet vaporization. Such analysis is still not in place, which motivates the present study.

The paper is organized as follows. In Section 2, the transient formulation for droplet vaporization is solved analytically with the help of appropriate coordinate transformations. The characteristic times for droplet heating and vaporization are derived through the matching conditions. The matching conditions and the Clausius-Clapeyron relation on the droplet surface are solved with the help of those analytical solutions and appropriate evaluation of various thermodynamic and transport properties. In Section 3, a theoretical model is proposed, which interprets the time change of droplet size during its vaporization under wide ranges of temperature and pressure. Comparison with experimental results reported in the literature verifies the theoretical model. The duel effect of pressure upon the droplet lifetime is analyzed. The concluding remarks are given in Section 4.

2. Formulation

We consider a single-component, volatile droplet in a stagnant environment of hot nitrogen with constant and uniform pressure. Since the droplet heating and vaporization take place simultaneously, the formulation for the droplet vaporization process involves mass and energy conservation for both droplet (the liquid phase) and the ambience (the gaseous mixture of fuel vapor and nitrogen) as well as their balance relations across the liquid-gas interface (droplet surface) [22]. The governing equations for gas phase system consist of transport of volatile species, denoted by subscript F and the conservation of energy (in terms of temperature distribution). At the initial instant, no fuel is evaporated and thereby the fuel mass fraction is $Y_F(t=0,\ r)=0$ in the gaseous environment, and both the droplet and the ambience have uniform temperatures, denoted by T_0 and T_∞, respectively. As vaporization proceeds, the thermodynamic equilibrium at the evaporating interface is characterized by the Clausius-Clapeyron relation, which correlates the droplet surface temperature, denoted by $T_s=T(r_s,t)$, with the local mass fraction of the evaporated fluid, denoted by $Y_{Fs}=Y_F(r_s,t)$.

2.1. Governing equations

For analytical convenience, we assume that the density-weighted mass diffusion coefficients, ρD, thermal conductivities, λ, and heat capacities at constant pressure of both gas and liquid phases, c_{pg} and c_{pl}, are constants. In gas phase, the mass conservation equations for the fuel vapor and inert gas are given by

$$\frac{\partial Y_F}{\partial t}+v\frac{\partial Y_F}{\partial r}=D_g\frac{1}{r^2}\frac{\partial}{\partial r}\left(r^2\frac{\partial Y_F}{\partial r}\right),\ \ Y_N=1-Y_F \tag{1}$$

where v is the Stefan flow velocity relative to the droplet surface, and D_g is the mass diffusion coefficient of the gaseous mixture. The energy conservation equation for gaseous mixture is given by

$$\frac{\partial T_g}{\partial t}+v\frac{\partial T_g}{\partial r}=Le_gD_g\frac{1}{r^2}\frac{\partial}{\partial r}\left(r^2\frac{\partial T_g}{\partial r}\right) \tag{2}$$

where the Lewis number is defined as $Le_g=\lambda_g/(\rho_g c_{pg}D_g)$. Since the droplet is placed in the quiescent environment, the internal flow would be inconsiderable, thus, the energy equation for liquid phase is given by

$$\frac{\partial T_l}{\partial t}=Le_lD_l\frac{1}{r^2}\frac{\partial}{\partial r}\left(r^2\frac{\partial T_l}{\partial r}\right) \tag{3}$$

where D_l is the mass diffusion coefficient of the liquid and Le_l is analogously defined as $Le_l=\lambda_l/(\rho_l c_{vl}D_l)$.

The initial and boundary conditions for those governing equations are specified as

$t=0:$	$Y_F=0,\ \ T_g=T_\infty,\ \ T_l=T_0$	(Ic-1)
$r=0:$	$\partial T_l/\partial r=0$	(Bc-1)
$r=r_s(t):$	$Y_F=Y_{Fs}(t),\ \ T_g=T_s(t),\ \ T_l=T_s(t)$	(Bc-2)
$r\to\infty:$	$Y_F=0,\ \ T_g=T_\infty$	(Bc-3)

where $r_s(t)$ refers to the temporally varying droplet radius.

Nevertheless, the governing equations are not in closed form because the surface-related quantities, i.e., $Y_{Fs}(t)$, $T_s(t)$, and $r_s(t)$, remain to be determined through the matching conditions at the evaporating interface. The fuel vapor on the droplet surface is partially transported by Stefan flow to downstream and the rest by diffusion to far field. Thereby the mass balance relation is given by

$$\dot{m}_F=\dot{m}_FY_{Fs}-4\pi\rho_gD_gr_s^2\left(\frac{\partial Y_F}{\partial r}\right)_{r=r_s} \tag{4}$$

where the loss of droplet mass is related to the reduction of radius, i.e., $\dot{m}_F=-4\pi\rho_lr_s^2dr_s/dt$. Meanwhile, energy is transferred from the hot ambience to the droplet surface, partially contributing to the droplet warm-up and the rest providing energy to sustain the vaporization process. Consequently, the energy balance is given by

$$4\pi\lambda r_s^2\left(\frac{\partial T_g}{\partial r}\right)_{r=r_s}=\dot{m}_FL+4\pi\lambda_lr_s^2\left(\frac{\partial T_l}{\partial r}\right)_{r=r_s} \tag{5}$$

where L is the enthalpy of vaporization for the droplet fluid.

We assume that the vaporization occurs at thermodynamically equilibrium state. Therefore, on the droplet surface, the relationship between mass fraction of fuel vapor and temperature is determined by the Clausius-Clapeyron relation, i.e.,

$$\frac{Y_{Fs}/W_F}{Y_{Fs}/W_F+(1-Y_{Fs})/W_N}=\frac{p_n}{p}\exp\left[\frac{L(T_s)}{R}\left(\frac{1}{T_{b,n}}-\frac{1}{T_s}\right)\right] \tag{6}$$

where W is the molar mass of each species, T_{bn} the boiling point temperature of the droplet fluid under the normal pressure p_n. Supplementing the matching conditions and phase equilibrium relation to the governing equations, the mathematical formulation of the droplet vaporization problem is in closed form, and hence the solution procedure could be initiated.

2.2. Solutions to the gas phase

The evaporation results in droplet radius shrinking. For mathematical convenience in dealing with the moving boundary problem, we introduce a scaled coordinate in analogy to that adopted by Law and Sirignano [29], i.e.,

$$\sigma=\frac{r}{r_s(t)},\ \ \tau=\int_0^t\frac{D_g}{r_s^2(t')}dt' \tag{7}$$

Writing Eqs. (1) and (2) in the scaled coordinate (7), we have

$$\frac{\partial Y_F}{\partial \tau} - \frac{1}{2}\left(\frac{1}{\sigma^2}\frac{\rho_l}{\rho_g} + \sigma\right)\frac{1}{D_g}\frac{dr_s^2}{dt}\frac{\partial Y_F}{\partial \sigma} = \frac{1}{\sigma^2}\frac{\partial}{\partial \sigma}\left(\sigma^2\frac{\partial Y_F}{\partial \sigma}\right) \tag{8}$$

$$\frac{\partial T_g}{\partial \tau} - \frac{1}{2}\left(\frac{1}{\sigma^2}\frac{\rho_l}{\rho_g} + \sigma\right)\frac{1}{D_g}\frac{dr_s^2}{dt}\frac{\partial T_g}{\partial \sigma} = Le_g\frac{1}{\sigma^2}\frac{\partial}{\partial \sigma}\left(\sigma^2\frac{\partial T_g}{\partial \sigma}\right) \tag{9}$$

Replacing radial coordinate r by the normalized coordinate σ, the moving boundary effect is transformed into an equivalent convection term. The initial and boundary conditions for Eqs. (8) and (9) are specied as

$\tau = 0$	$Y_F = 0, \quad T_g = T_\infty$	(Ic-1')
$\sigma = 1$	$Y_F = Y_{Fs}(\tau), \quad T_g = T_s(\tau)$	(Bc-2')
$\sigma \to \infty$	$Y_F = 0, \quad T_g = T_\infty$	(Bc-3')

The first order derivatives impose substantial difficulties in delaing with Eqs. (8) and (9) analytically. Whereas, such mathematical issue could be alleviated by introducing the following coordinate transform

$$\xi_g = \left[\int_1^\infty F_g(\sigma')d\sigma'\right]^{-1}\int_1^\sigma F_g(\sigma')d\sigma' \tag{10}$$

where

$$F_g(\sigma) = \exp\left\{-\int_1^\sigma\left[\frac{2}{\sigma'} + \frac{1}{2}\left(\frac{1}{\sigma'^2}\frac{\rho_l}{\rho_g} + \sigma'\right)\frac{1}{D_g}\frac{dr_s^2(t)}{dt}\right]d\sigma'\right\} \tag{11}$$

By chain's rule, the first and second order derivatives with respect to σ_s can be written in the terms of ξ_g as

$$\frac{\partial}{\partial \sigma_s} = \frac{\partial \xi_g}{\partial \sigma_s}\frac{\partial}{\partial \xi_g}$$

$$\frac{\partial^2}{\partial \sigma_s^2} = \frac{d^2\xi_g}{d\sigma_s^2}\frac{\partial}{\partial \xi_g} + \left(\frac{d\xi_g}{d\sigma_s}\right)^2\frac{\partial^2}{\partial \xi_g^2}$$

Applying the coordination transformation (10) to Eqs. (8) and (9), we have

$$\frac{\partial Y_F}{\partial \tau} = D_{\text{eff}}\frac{\partial^2 Y_F}{\partial \xi_g^2}, \quad \frac{\partial T_g}{\partial \tau} = Le_g D_{\text{eff}}\frac{\partial^2 T_g}{\partial \xi_g^2} \tag{12}$$

where the effective diffusion coefficient is defined as

$$D_{\text{eff}} = \left\{F_g(\sigma)\left[\int_1^\infty F_g(\sigma')d\sigma'\right]^{-1}\right\}^2 \tag{13}$$

It is a function of σ and thus varies with ξ_g. On the droplet surface where evaporation occurs, the solutions for Y_F and T are to be substituted into the matching conditions. The matching conditions refer to Eqs. (4) – (6) that describe the mass conservation, energy conservation and phase equilibrium relation between the fuel vapor and its condensed phase at the droplet surface. This implies that the accuracy of the solutions for Y_F and T remote from the droplet surface has insignificant impact upon determination of the droplet vaporization rate, which relies upon the analysis at evaporating interface. It allows us to choose a representative value for D_{eff} that characterizes its contirbution to Y_{Fs} and T_s evaluated by their analytical solutions to Eqs. (8) and (9). Accordingly, we may specify the characteristic effective diffusion coefficient on the droplet surface where $\sigma = 1$, giving

$$D_{\text{eff}}^c = \left[\int_1^\infty F(\sigma')d\sigma'\right]^{-2} \tag{14}$$

The boundary conditions are revised as

$\xi_g = 0:$	$Y_F = Y_{Fs}(\tau), \quad T_g = T_s(\tau)$	(Bc-2'')
$\xi_g = 1:$	$Y_F = 0, \quad T_g = T_\infty$	(Bc-3'')

With the help of $D_{\text{eff}}^c D_{\text{eff}}$, the Eq. (12) could be solved analytically subject to the initial condition (Ic-1') and boundary conditions (Bc-2'') and (Bc-3''), giving

$$Y_F(\xi_g, \tau) = Y_{Fs}(\tau) - \xi_g Y_{Fs}(\tau) + 2\sum_{n=1}^\infty \sin(n\pi x)e^{-D_{\text{eff}}^c n^2\pi^2\tau}R_n^Y(\tau) \tag{15}$$

$$T_g(\xi_g, \tau) = T_s(\tau) + \xi_g[T_\infty - T_s(\tau)] + 2\sum_{n=1}^\infty \sin(n\pi x)e^{-Le_g D_{\text{eff}}^c n^2\pi^2\tau}R_n^T(\tau) \tag{16}$$

where $R_n^Y(\tau)$ and $R_n^T(\tau)$ are

$$R_n^Y(\tau) = -\frac{1}{n\pi}\left(\frac{\partial Y_{Fs}}{\partial \tau}\frac{e^{D_{\text{eff}}^c n^2\pi^2\tau} - 1}{D_{\text{eff}}^c n^2\pi^2} - \int_0^t \frac{e^{D_{\text{eff}}^c n^2\pi^2\tau} - 1}{D_{\text{eff}}^c n^2\pi^2}\frac{\partial^2 Y_{Fs}}{\partial \tau^2}d\tau\right) \tag{17}$$

$$R_n^T(\tau) = \int_0^1 T_\infty \sin(n\pi\xi_g)d\xi_g - \frac{1}{n\pi}\left[T_s(0) - (-1)^n T_\infty\right] - \frac{1}{n\pi}\left(\frac{\partial T_s}{\partial \tau}\frac{e^{Le_g D_{\text{eff}}^c n^2\pi^2\tau} - 1}{Le_g D_{\text{eff}}^c n^2\pi^2} - \int_0^t \frac{e^{Le_g D_{\text{eff}}^c n^2\pi^2\tau} - 1}{Le_g D_{\text{eff}}^c n^2\pi^2}\frac{\partial^2 T_s}{\partial \tau^2}d\tau\right) \tag{18}$$

On the droplet surface, the fuel vapor is transported to the ambience by convection and diffusion (loss contribution) and meanwhile supplied by continuous evaporation from liquid droplet (gain contribution). Therefore, we argue that dynamic equilibrium is maintained on the droplet surface. It implies that except at a very brief period, during which the phase equilibrium condition is established, the time change of Y_{Fs} tends to be inconsiderable than the unsteadiness resulting from the droplet heating in vaporization process [30, 31]. The same argument applies to the droplet surface temperature T_s according to the Clausius-Clapeyron relation, and accordingly, we can neglect the terms containing the second order derivatives of Y_{Fs} and T_s in Eqs. (17) and (18). Substituting those simplifications into Eqs. (15) and (16) yields the following solutions for Y_F and T_g

$$Y_F(\xi_g, \tau) = Y_{Fs}(\tau) - \xi_g Y_{Fs}(\tau) - \frac{2}{D_{\text{eff}}^c}\frac{\partial Y_{Fs}}{\partial \tau}\sum_{n=1}^\infty \frac{\sin(n\pi\xi_g)}{n^3\pi^3} + \frac{2}{D_{\text{eff}}^c}\frac{\partial Y_{Fs}}{\partial \tau}\sum_{n=1}^\infty \frac{\sin(n\pi\xi_g)e^{-D_{\text{eff}}^c n^2\pi^2\tau}}{n^3\pi^3} \tag{19}$$

$$T_g(\xi_g, \tau) = T_s(\tau) + \xi_g[T_\infty - T_s(\tau)] - \frac{2}{Le_g D_{\text{eff}}^c}\frac{\partial T_s}{\partial \tau}\sum_{n=1}^\infty \frac{\sin(n\pi\xi_g)}{n^3\pi^3} + 2\sum_{n=1}^\infty \frac{\sin(n\pi\xi_g)}{n\pi}e^{-Le_g D_{\text{eff}}^c n^2\pi^2\tau}\left[T_\infty - T_s(0) + \frac{1}{n^2\pi^2 Le_g D_{\text{eff}}^c}\frac{\partial T_s}{\partial \tau}\right] \tag{20}$$

On the droplet surface where $\sigma = 1$, the derivatives of Y_F and T_g with respect to σ shall be calculated through chain's rule, i.e.,

$$\left(\frac{\partial Y_F}{\partial \sigma}\right)_{\sigma=1} = \left(\frac{\partial Y_F}{\partial \xi_g}\right)_{\xi=0}\left(\frac{d\xi_g}{d\sigma}\right)_{\sigma=1}$$

$$\left(\frac{\partial T_g}{\partial \sigma}\right)_{\sigma=1} = \left(\frac{\partial T_g}{\partial \xi_g}\right)_{\xi=0}\left(\frac{d\xi_g}{d\sigma}\right)_{\sigma=1} \tag{21}$$

With the help of Eq. (10) and evaluating the derivatives of Eqs. (19) and (20), we have

$$\left(\frac{\partial Y_F}{\partial \sigma}\right)_{\sigma=1} = -\left[Y_{Fs}(\tau) + \frac{1}{3}\frac{1}{D^c_{\text{eff}}}\frac{\partial Y_{Fs}}{\partial \tau}\left(1 - e^{-D^c_{\text{eff}}\pi^2\tau}\right)\right]\left[\int_1^\infty F_g(\sigma)d\sigma\right]^{-1} \tag{22}$$

$$\left(\frac{\partial T_g}{\partial \sigma}\right)_{\sigma=1} = \left\{T_\infty - T_s(\tau) - \frac{1}{3}\frac{1}{Le_g D^c_{\text{eff}}}\frac{\partial T_s}{\partial \tau}\left(1 - e^{-Le_g D^c_{\text{eff}}\pi^2\tau}\right) + [T_\infty - T_s(0)]\left[\vartheta_3\left(e^{-Le_g D^c_{\text{eff}}\pi^2\tau}\right) - 1\right]\right\}\left[\int_1^\infty F_g(\sigma)d\sigma\right]^{-1} \tag{23}$$

where ϑ refers to the elliptic theta function. Since the quasi-steady state in gas phase establishes swiftly during the droplet vaporization, we make the subsequent approximation

$$\sum_{n=1}^{\infty}\frac{e^{-Le_g D^c_{\text{eff}} n^2\pi^2\tau}}{n^2\pi^2} \to e^{-Le_g D^c_{\text{eff}}\pi^2\tau}\sum_{n=1}^{\infty}\frac{1}{n^2\pi^2} = \frac{1}{6}e^{-Le_g D^c_{\text{eff}}\pi^2\tau} \tag{24}$$

during derivation of Eqs. (22) and (23).

Known the integral of $F_g(\sigma)$ from 1 to $\sigma = \infty$, the characteristic value of effective diffusion coefficient can be calculated, and subsequently the determination of $(\partial Y_F/\partial\sigma)_{\sigma=1}$ and $(\partial T_g/\partial\sigma)_{\sigma=1}$ according to Eqs. (22) and (23). Analyzing Eq. (11), it is noted that the linear term $(\sigma/D_g)(dr_s^2/dt)$ actually results from the coordinate transformation from the (r, t)- to (σ, τ)-space. When approaching to the end of the droplet vaporization, i.e., $r_s \to 0$, the coordinate σ, according to Eq. (7), becomes exceedingly large, even for moderate radial distance r. Such pure mathematical effect leads to the divergence of the $F_g(\sigma)$ at large values of σ, and has no contribution to the physical interpretation of the droplet vaporization process. Thereby, we remove this linear term in the estimation of the integral of $F_g(\sigma)$, yielding

$$\int_1^\infty F(\sigma)d\sigma \approx \int_1^\infty \exp\left\{-\int_1^\sigma\left[\frac{2}{\sigma'} + \frac{1}{2}\frac{1}{\sigma'^2}\frac{\rho_l}{\rho_g}\frac{1}{D_g}\frac{dr_s^2(t)}{dt}\right]d\sigma'\right\}d\sigma = \frac{1}{a_g}\left(e^{a_g} - 1\right) \tag{25}$$

where a_g is

$$a_g = -\frac{1}{2}\frac{1}{D_g}\frac{dr_s^2}{dt}\frac{\rho_l}{\rho_g} > 0 \tag{26}$$

Substituting Eq. (25) into Eqs. (22) and (23), we obtain

$$\left(\frac{\partial Y_F}{\partial \sigma}\right)_{\sigma=1} = -\left[Y_{Fs}(\tau) + \frac{1}{3}\frac{1}{D^c_{\text{eff}}}\frac{\partial Y_{Fs}}{\partial \tau}\left(1 - e^{-D^c_{\text{eff}}\pi^2\tau}\right)\right]\frac{a_g}{e^{a_g} - 1} \tag{27}$$

$$\left(\frac{\partial T_g}{\partial \sigma}\right)_{\sigma=1} = \left\{T_\infty - T_s(\tau) - \frac{1}{3}\frac{1}{Le_g D^c_{\text{eff}}}\frac{\partial T_s}{\partial \tau}\left(1 - e^{-Le_g D^c_{\text{eff}}\pi^2\tau}\right) + [T_\infty - T_s(0)]\left[\vartheta_3\left(e^{-Le_g D^c_{\text{eff}}\pi^2\tau}\right) - 1\right]\right\}\frac{a_g}{e^{a_g} - 1} \tag{28}$$

Eqs. (27) and (28) are to be substituted into the mass and energy balance relations on the droplet surface, respectively.

2.3. Solutions to the liquid phase

By defining $T = rT_l$, Eq. (3) can be written in the form of one-dimensional heat conduction in Cartesian coordinate, i.e.,

$$\frac{\partial T}{\partial t} = D_l Le_l\frac{\partial^2 T}{\partial r^2} \tag{29}$$

Applying the coordinate transform (7) to Eq. (29), we have

$$\frac{\partial T}{\partial \tau} - \frac{1}{2}\frac{\sigma}{D_g}\frac{dr_s^2(t)}{dt}\frac{\partial T}{\partial \sigma} = \frac{Le_l D_l}{D_g}\frac{\partial^2 T}{\partial \sigma^2} \tag{30}$$

In analogy to Eq. (10), we define a new coordinate ξ_l as

$$\xi_l = \frac{\text{erfi}(\sqrt{a_l}\sigma)}{\text{erfi}(\sqrt{a_l})} \tag{31}$$

where "erfi" refers to the imaginary error function, and the factor a_l is defined as

$$a_l = -\frac{1}{4}\frac{1}{D_l Le_l}\frac{dr_s^2}{dt} \tag{32}$$

Applying the coordinate transform (31) to Eq. (30), the first order derivative no longer appears, giving

$$\frac{\partial T}{\partial \tau} = \lambda_{l,\text{eff}}\frac{d^2 T}{d\xi_l^2} \tag{33}$$

where the effective heat conduction coefficient denotes for

$$\lambda_{l,\text{eff}} = \left[\frac{1}{e^{-a_l\sigma^2}}\frac{\sqrt{\pi}\,\text{erfi}(\sqrt{a_l})}{2\sqrt{a_l}}\right]^{-2}\frac{D_l Le_l}{D_g} \tag{34}$$

Following the same procedure as we derive D^c_{eff}, the characteristic value for effective heat conduction coefficient, denoted by $\lambda^c_{l,\text{eff}}$, can be specified by setting $\sigma = 1$. The initial and boundary conditions for Eq. (33) are

$\tau = 0$	$T = \sigma(\xi_l) r_0 T_0$	(Ic-i)
$\xi_l = 0$	$T = 0$	(Bc-ii)
$\xi_l = 1$	$T = r_s(\tau)T_s(t)$	(Bc-iii)

where r_0 is the initial radius of the droplet.

The functional relationship between σ and ξ_l shall be obtained by inversely solving Eq. (31), formally yielding

$$\sigma = -\frac{i\,\text{erf}^{-1}[i\xi_l\,\text{erfi}(\sqrt{a_l})]}{\sqrt{a_l}} \tag{35}$$

where erf^{-1} denotes the inverse function of error function. Eq. (32) shows that a_l involves the surface regression rate of the evaporating droplet, dr_s^2/dt, which can be considered as a small quantity during droplet vaporization. This implies that the right-hand side of Eq. (35) can be approximated by power series in terms of a_l, giving

$$\sigma = \xi_l + \frac{1}{3}\left(\xi_l - \xi_l^3\right)a_l + O\left(a_l^2\right) \tag{36}$$

The initial condition (Ic-i) is accordingly modified to

$\tau = 0$	$T = [\xi_l + \frac{a_l}{3}(\xi_l - \xi_l^3)] r_0 T_0$	(Ic-i')

which we shall adopt in the subsequent solution of the liquid phase system.

Equating the effective heat conduction coefficient to its characteristic value, Eq. (33) can be solved analytically subject to the initial condition (Ic-i') and boundary conditions (Bc-ii) and (Bc-iii), giving

$$T(\xi_l, \tau) = \left[\xi_l + \frac{a_l}{3}\left(\xi_l - \xi_l^3\right)\right]r_s(\tau)T_s(\tau) + 2\sum_{n=1}^{\infty}\sin(n\pi\xi_l)R_{n,l}(\tau)e^{-\lambda^c_{l,\text{eff}}n^2\pi^2\tau} \tag{37}$$

where, considering the dynamic equilibrium on the droplet surface, the quantity $R_{n,\,l}$ can be written as

$$R_{n,l}(\tau) = \frac{2a_l(-1)^{n+1}}{n^3\pi^3}T_0 r_0 + (-1)^n\frac{e^{\lambda^c_{l,\text{eff}}n^2\pi^2\tau} - 1}{\lambda^c_{l,\text{eff}}n^3\pi^3}\frac{d}{d\tau}[r_s(\tau)T_s(\tau)] \tag{38}$$

2.4. Analysis on the droplet surface

The mass balance relation on the interface in the scaled coordinate (τ, σ) is given by

$$\frac{\rho_l}{\rho_g}\frac{1}{D_g}\frac{dr_s^2}{dt}(1-Y_{Fs}) = 2\left(\frac{\partial Y_F}{\partial \sigma}\right)_{\sigma=1} \tag{39}$$

After a swift induction period in the order of $O(1/D_{\text{eff}}^c\pi^2)$, the gas phase unsteadiness decays to be negligible. Accordingly, we can remove the exponentially decaying term in the coefficient of dY_{Fs}/dt in Eq. (27), giving,

$$\left(\frac{\partial Y_F}{\partial \sigma}\right)_{\sigma=1} = -\left(Y_{Fs} + \frac{1}{3}\frac{1}{D_{\text{eff}}^c}\frac{\partial Y_{Fs}}{\partial \tau}\right)\frac{a_g}{e^{a_g}-1} \tag{40}$$

Substituting into Eq. (39), we obtain an ordinary differential equation for the temporal variation of Y_{Fs}, i.e.,

$$\frac{\partial Y_{Fs}}{\partial \tau} = -3D_{\text{eff}}^c(e^{a_g}Y_{Fs} + 1 - e^{a_g}) \tag{41}$$

The droplet size changes slightly during the initial build-up of fuel vapor and the elevation of droplet surface temperature, which implies that the quantity a_g, given by Eq. (26), could be considered as a constant. Solving Eq. (41) subject to the initial condition of $Y_{Fs}(0) = 0$, it yields

$$Y_{Fs} = \left(1-e^{-a_g}\right)\left(1-e^{-3e^{a_g}D_{\text{eff}}^c\tau}\right) \tag{42}$$

It is seen that after an induction period characterized by $1/3e^{a_g}D_{\text{eff}}^c$, Eq. (42) asymptotes to

$$Y_{Fs}^0 = 1 - e^{-a_g} \tag{43}$$

When the droplet is exposed in the hot environment, the fuel vapor starts to accumulate at the droplet surface due to vaporization. Then, Y_{Fs}^0 represents final stage of fuel vapor accumulation, subsequent to which, the mass fraction of fuel vapor at the droplet surface almost remains unchanged. The rate of fuel vapor generation from vaporization tends to balance with the transport of fuel vapor at the droplet surface through diffusion, i.e., the vaporization could be regarded as in quasi-steady state. With the knowledge of droplet surface regression rate, i.e., dr_s^2/dt, which we shall discuss subsequently, the factor a_g could be calculated and hence the asymptotic mass fraction Y_{Fs}^0 could be determined. Substituting Y_{Fs}^0 into the Clausius-Clapeyron relation, given by Eq. (6), the asymptotic temperature on the droplet surface can be obtained as

$$T_s^0 = T_{bn}\left(1 + \frac{RT_{bn}}{L\left(T_s^0\right)}\left\{\ln\frac{p_n}{p} + \ln\left[1 + \frac{W_F}{W_N(e^{a_g}-1)}\right]\right\}\right)^{-1} \tag{44}$$

For droplet evaporating at high temperature and pressure conditions, the quasi-steady vaporization is preceded by a heating stage. During the heating stage, vaporization rate tends to be indiscernible compared with that in the subsequent stage of quasi-steady vaporization. The time required to heat the droplet to a uniform temperature T_s^0 can be determined by

$$\frac{4\pi r_0^3}{3}\rho_l c_{vl}\left(T_s^0 - T_0\right) = \int_0^{t'_{\text{heating}}} 4\pi r_0^2\lambda_g\left(\frac{\partial T_g}{\partial \sigma}\right)_{\sigma=1} dt \tag{45}$$

Eq. (45) can be considered as a simplified model for droplet heating time. The left-hand side is the energy required to increase the droplet temperature uniformly from T_0 to the final stage T_s^0 subsequent to which the quasi-steady vaporization dominates over the droplet heating. The integrand on right-hand side represents the heating power at the droplet surface due to heat conduction from the hot environment, and hence the upper limit of the integral refers to an estimate to the heating time. Solving Eq. (45), one obtains,

$$t'_{\text{heating}} = \frac{c_{vl}\rho_l r_0^2}{3\lambda_g}\frac{T_s^0 - T_0}{T_\infty - T_s^0} \tag{46}$$

However, it has been indicated that the temperature at the droplet center tends to be considerably lower than T_s^0 when considerable evaporation initiates subsequent to the heating stage. Therefore, the t'_{heating} tends to overestimate the duration of the heating stage. The rigorous determination of the droplet temperature gradient inside the droplet could be dealt with by analyzing the temporal and spatial evolution of T_l derived from Eq. (37). Alternatively, Snegirev proposed a few models that interprets the droplet temperature profiles as power-law or polynomial functions of radial coordinates [36]. For simplicity and illustrative concern, we assume that the droplet temperature can be approximated by a linear function of radial coordinate, i.e., $T_l^o(r) \approx T_0 + (T_s^0 - T_0)r/r_0$, when the droplet enters the quasi-steady vaporization stage. Accordingly, the energy required to heat the droplet with uniform temperature T_0 to the particular temperature profile given by T_l^o can be evaluated by

$$\Delta Q = 4\pi c_{vl}\int_0^{r_0} r^2\left[T_0 + \left(T_s^0 - T_0\right)\frac{r}{r_0}\right]dr - \frac{4}{3}\pi r_0^3 c_{vl}T_0 = \pi r_0^3 c_{vl}\left(T_s^0 - T_0\right) \tag{47}$$

Comparing with Eq. (45), the heating time can be approximately evaluated as

$$t_{\text{heating}} = \frac{3}{4}t'_{\text{heating}} = \frac{c_{vl}\rho_l r_0^2}{4\lambda_g}\frac{T_s^0 - T_0}{T_\infty - T_s^0} \tag{48}$$

In the quasi-steady vaporization stage, the heat transfer from the hot ambience is mainly utilized to evaporate the droplet, thus the energy balance relation can be revised from Eq. (5) by removing the heating effect, giving

$$\left(\frac{\partial T_g}{\partial \sigma}\right)_{\sigma=1} = -\frac{1}{2}\frac{\rho_l}{\lambda_g}\frac{dr_s^2(t)}{dt}L(T_s) \tag{49}$$

Substituting $(\partial T_g/\partial\sigma)_{\sigma=1}$ from Eq. (28) into Eq. (49), we obtain an ordinary differential equation for r_s^2, which is analogous to the classic d^2-law characterizing the droplet vaporization, i.e.,

$$\frac{dr_s^2}{dt} = -\frac{2\rho_g D_g}{\rho_l}\ln\left[1 + \frac{Le_g c_{pg}\left(T_\infty - T_s^0\right)}{L\left(T_s^0\right)}\right] \tag{50}$$

Solving for time duration of quasi-steady vaporization, $t_{\text{vaporization}}$, we obtain

$$t_{\text{vaporization}} = \frac{1}{2}\frac{\rho_l r_0^2}{\rho_g D_g \ln\left[1 + Le_g c_{pg}\left(T_\infty - T_s^0\right)/L\left(T_s^0\right)\right]} \tag{51}$$

In terms of Eqs. (48) and (51), the overall droplet lifetime can be evaluated in the following explicit form:

$$t_{\text{total}} = t_{\text{heating}} + t_{\text{vaporization}} = \frac{\rho_l}{\rho_g}\frac{r_0^2}{D_g}\left\{\frac{1}{4Le_g}\frac{c_{vl}}{c_{pg}}\frac{T_s^0 - T_0}{T_\infty - T_s^0} + \frac{1}{2}\frac{1}{\ln\left[1 + Le_g c_{pg}\left(T_\infty - T_s^0\right)/L\left(T_s^0\right)\right]}\right\} \tag{52}$$

Acquiring the surface regression rate, given by Eq. (50), the asymptotic droplet surface temperature, according to Eq. (44), can be written in the subsequent form

$$T_s^0 = T_{bn}\left(1 + \frac{RT_{bn}}{L\left(T_s^0\right)}\left\{\ln\frac{p_n}{p} + \ln\left[1 + \frac{W_F L\left(T_s^0\right)}{W_N Le_g c_{pg}\left(T_\infty - T_s^0\right)}\right]\right\}\right)^{-1} \tag{53}$$

Therefore, T_s^0 shall be determined iteratively through Eq. (53) when the temperature dependence of enthalpy of vaporization is known.

2.5. Thermodynamic and transport properties

The enthalpy of vaporization can be directly solved through

$$L = \int_{V_m^l}^{V_m^v} \left[T\left(\frac{\partial p}{\partial T}\right)_{V_m} - p \right] dV_m + p_e\left(V_m^v - V_m^l\right) \tag{54}$$

where V_m^l and V_m^v denote the molar volumes of liquid and gas phase, respectively, and p_e is the equilibrium vapor pressure. Those equilibrium states can be iteratively calculated by simultaneously solving an equation of state that is accurate at both liquid and gas phase, e.g., Soave-Redich-Kwong or Peng-Robinson equation of states. It is acknowledged that Eq. (54) cannot interpret the temperature-dependence of enthalpy of vaporization in a mathematically explicit form.

Fortunately, the enthalpy of vaporization can also be evaluated through an analytical formula [41], given by

$$\frac{L}{L_R} = \left[1 - f_E\left(\frac{q_{l,R}}{2} - 1\right)t_L\right]^{1-t_L}\left[f_E\frac{q_{l,R}}{2(1-\alpha)}(1-t_L)^{1-\alpha} + \left(1 - \frac{1}{2}f_E q_{l,R}\right)(1-t_L)^{\beta}\right]^{t_L} \tag{55}$$

where L_R is the enthalpy of vaporization at reference temperature T_R. The α and β are the critical exponents characterizing the heat capacity at constant volume and the density difference when the fluid is close to its thermodynamic critical state, i.e., $c_v \sim (T_c - T)^{-\alpha}$ and $\rho_l - \rho_c \sim (T_c - T)^{\beta}$. The literature on the critical phenomena suggests that the approximate values of α of β for various fluids are 0.1096 and 0.3265, respectively [42]. According to the X-ray scattering experimental studies on liquid configurations, the coordination number, denoted by q, changes in a restricted range between 9 and 11 for most fluids [43]. Since the reference state is remote from the critical point, reference coordination number, $q_{l,R}$, tends to be greater in magnitude, which leads us to specify $q_{l,R} = 11$ in the subsequent discussion. The energy factor f_E and normalized temperature t_L are defined in terms of reference and critical temperatures

$$f_E = \frac{R(T_c - T_R)}{L_R}, \quad t_L = \frac{T - T_R}{T_c - T_R} \tag{56}$$

Therefore, with the knowledge of both reference state and critical temperature, i.e., L_R and T_c, the enthalpy of vaporization can be calculated through Eq. (55) at the surface temperature T_s^0. Preceding to the solution of droplet vaporization system, the thermodynamic and transport properties in both gas and liquid phases, e.g., density, heat capacity, mass and thermal conductivities, must be determined. The specification of those quantities is given in the Appendix. Substituting those specified thermodynamic and transport properties into Eqs. (48), (51), and (52), the characteristic time scales of droplet vaporization, i.e., t_{heating}, $t_{\text{vaporization}}$ and t_{total}, can be readily calculated.

3. Results and discussion

Assuming that the quasi-steady state vaporization occurs at thermodynamic equilibrium condition, the asymptotic temperature at the droplet surface, T_s^0, would be close to the wet-bulb temperature [28,30], which is usually considerably lower than the boiling point at the current pressure. Due to lack of an accurate theoretical means to calculate the wet-bulb temperature, Miller et al. [44] proposed the following empirical correlation to the experimental results for a variety of fuels in terms of the boiling temperature of the specific liquid and the environmental temperature:

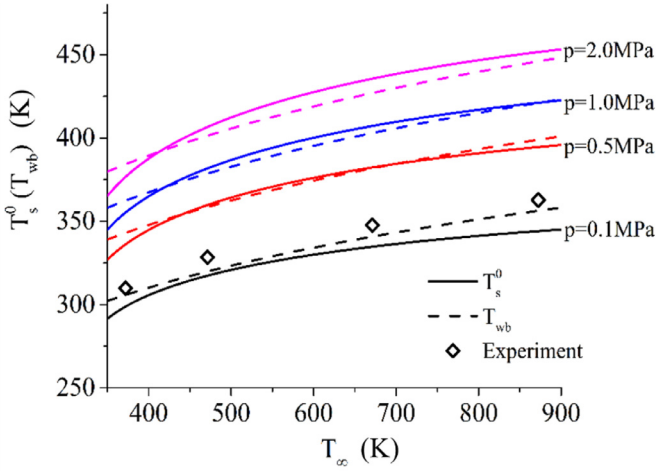

Fig. 1. Comparison of asymptotic droplet surface temperature T_s^0 (solid lines) with the wet-bulb temperature T_{wb} estimated by the fitting formula Eq. (57) (dashed lines). The hollow symbols represent the experimentally determined wet-bulb temperature of heptane droplet at normal pressure from Ref. [45]

$$T_{wb} = 137\left(\frac{T_b}{373.15}\right)^{0.68}\log(T_g) - 45 \tag{57}$$

In the present model, T_s^0 could be determined by iteratively solving Eq. (53), in which the thermodynamic and transport properties are evaluated by means of 1/3 rule and the enthalpy of vaporization by Eq. (55). Fig. 1 indicates that the calculated droplet surface temperature based on our theoretical model agrees well with the wet-bulb temperatures estimated by Eq. (57) as well as those measured in experiments for atmospheric pressure [45].

With the knowledge of T_s^0, the heating and vaporization times can be explicitly determined from Eq. (48) and Eq. (51), respectively, and hence the droplet lifetime by Eq. (52). Nomura et al. [6] defined an unsteadiness factor as the ratio of droplet heating time to its lifetime, i.e.,

$$\Phi_{\text{i}} = \frac{t_{\text{heating}}}{t_{\text{total}}} \tag{58}$$

It is seen that the droplet surface temperature grows with increasing either temperature or pressure of the environmental gas. It implies that more heat is required to warm up the droplet before its arrival at the quasi-steady vaporization state, and accordingly, the unsteadiness in the droplet vaporization process becomes more pronounced.

To verify the present theoretical analysis, we specify our conditions identical to those in Nomura et al.'s experiments [6], which considered an n-heptane droplet vaporizing at nitrogen environment under microgravity condition. In experiments, the droplet was suspended by a thin fiber, thus the overall droplet vaporization lifetime must be extrapolated from the droplet size history to its vanishing point. In Fig. 2, the scaled vaporization lifetimes (divided by the square of the initial droplet diameter), calculated by Eq. (52) at various temperatures and pressures, are compared with those extrapolated from experimental data. It shows that the theoretical model can accurately predict the droplet lifetime in wide ranges of temperature and pressure.

Both theoretical model and experimental results indicate that the droplet lifetime decreases with the ambient temperature. More interestingly, the results in Fig. 2 show that the droplet lifetime depends upon the ambient pressure in a non-monotonic manner. At low to moderate temperatures with $T_\infty < 510$K, the droplet lifetime becomes slightly longer when the ambient pressure is elevated from 0.1MPa to 0.5MPa. As pressure increasing from 0.5MPa

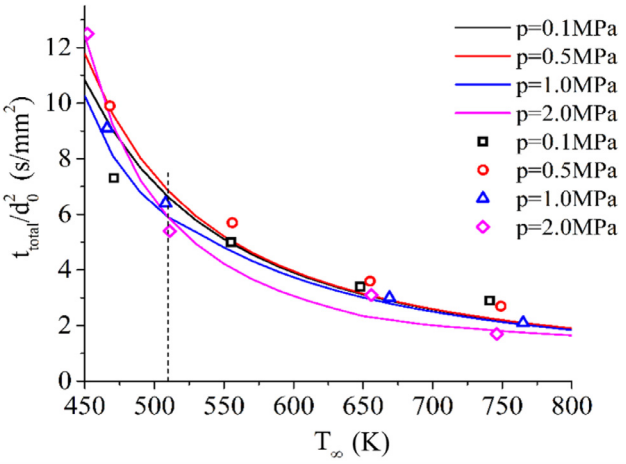

Fig. 2. Comparison of droplet lifetime calculated by theoretical model (solid lines) and those extrapolated from experimental data (denoted by hollow symbols) in [6].

to 1.0MPa, the droplet lifetime undergoes discernible reduction. By further increasing ambient pressure from 1.0MPa to 2.0MPa, the droplet lifetime tends to be significantly prolonged. However, at moderate to high temperatures with $T_\infty > 510$K, the droplet lifetimes for $p = 2.0$MPa are uniformly lower than those situations with lower ambient pressures. These results imply that the ambient pressure has both facilitating and impeding effects upon droplet vaporization. Moreover, the facilitating effect tends to dominate over the impeding effect when the ambient pressure becomes sufficiently high. It can be attributed to the competition between t_{heating} and $t_{\text{vaporization}}$ as increasing the ambient pressure.

According to Fig. 1 the droplet surface temperature gets higher as pressures. It results in the lengthening of the heating time, which partially contributes to the increase of droplet lifetime. Meanwhile, at low to moderate temperatures, e.g., $T_\infty < 510$ K, the discrepancy between T_s^0 and T_∞ tends to be moderate, which allows us to assume that $c_{pg}(T_\infty - T_s^0) \ll L(T_s^0)$. Consequently, the vaporization time could be simplified to

$$t_{\text{vaporization}} \approx \frac{1}{2}\frac{r_0^2\rho_l L(T_s^0)}{\lambda_g(T_\infty - T_s^0)} \tag{59}$$

Besides, the surface temperature T_s^0 must be remote from the critical temperature, leading to that according to ref [41], the enthalpy of vaporization could be represented by

$$\frac{L(T_s^0)}{L_0} \approx 1 - f_E\left(\frac{q_{l,R}}{2} - 1\right)\frac{T_s^0 - T_R}{T_c - T_R} \tag{60}$$

where the energy factor f_E, for the current n-heptane fuel is around 0.055. Taking derivative of $t_{\text{vaporization}}$ with respect to T_s^0 from Eq. (59) with simplified enthalpy of vaporization given by Eq. (60), we have

$$\frac{dt_{\text{vaporization}}}{dT_s^0} \approx \frac{1}{2}\frac{r_0^2\rho_l}{\lambda_g}\frac{L_R}{(T_\infty - T_s^0)^2}\left[1 - f_E\left(\frac{q_{l,R}}{2} - 1\right)\right] > 0 \tag{61}$$

where the reference temperature is 300 K. It can be interpreted as follows. At low to moderate temperatures, the heat transfer rate from the ambience to the droplet surface decreases as the surface temperature increasing, which lowers the temperature difference. Meanwhile, the decrement of vaporization enthalpy due to the same cause tends to be immaterial so that the vaporization rate is reduced. Thereby, the simultaneous increase of both heating and vaporization times results in a noticeably prolonged droplet lifetime at low to moderate temperatures, and it becomes more pronounced as ambient pressure grows. The decay of droplet lifetime at intermediate pressure, e.g., $p = 1.0$MPa might be attributed to the increment of λ_g and $\rho_g D_g$, whose temperature dependence is estimated by means of the 1/3 rule, given by Eq. (a4), in terms of the droplet surface temperature. According to Eqs. (48) and (51), both heating and vaporization times are shortened under the enhancement of transport properties.

At moderate to high temperatures, the logarithmic function in Eq. (51) cannot be estimated by its first order Taylor series. However, the dependence of vaporization time upon pressure, i.e., the behavior of $dt_{\text{vaporization}}/dT_s^0$, can still be interpreted by means of Eq. (59) because the logarithmic function has the same monotonicity as linear function. When the droplet surface temperature approaches to the critical temperature, according to Ref. [41], the enthalpy of vaporization can be evaluated through

$$\frac{L(T_s^0)}{L_R} \approx f_E\frac{q_{l,R}}{2(1-\alpha)}\left(\frac{T_c - T_s^0}{T_c - T_R}\right)^{1-\alpha} + \left(1 - \frac{1}{2}f_E q_{l,R}\right)\left(\frac{T_c - T_s^0}{T_c - T_R}\right)^{\beta} \tag{62}$$

Taking derivative of $t_{\text{vaporization}}$ with respect to T_s^0 from Eq. (59) with enthalpy of vaporization given by Eq. (62), we have

$$\frac{dt_{vaporization}}{dT_s^0} \approx \frac{1}{2}\frac{r_0^2\rho_l}{\lambda_g}\frac{L_0}{(T_\infty - T_s^o)^2}\left[\frac{1}{2}f_E q_{l,R}\left(\frac{T_c - T_s^o}{T_c - T_R}\right)^{1-\alpha}\left(\frac{1}{1-\alpha} - \frac{T_\infty - T_s^o}{T_c - T_s^o}\right) + \left(1 - \frac{1}{2}f_E q_{l,R}\right)\left(\frac{T_c - T_s^o}{T_c - T_R}\right)^{\beta}\left(1 - \beta\frac{T_\infty - T_s^o}{T_c - T_s^o}\right)\right] \tag{63}$$

When the environmental temperature is considerably higher than the critical temperature, T_s^0 becomes comparable with T_c. At conditions that $(T_\infty - T_s^0)/(T_c - T_s^0) > 1/\beta$, Eq. (63) indicates that $dt_{\text{vaporization}}/dT_s^0$ is negative and thereby the vaporization rate increases with the ambient pressure. This effect can be attributed to that the enthalpy of vaporization becomes exceedingly due to increasing of droplet surface temperature. The reduction of vaporization enthalpy renders the phase transition to occur more readily and hence accelerates the vaporization process.

At sufficiently high pressures, e.g., $p = 2.0$MPa, the reduction of vaporization time tends to compensate or even dominate over the lengthening of the heating time, leading to the uniform reduction of droplet lifetime. Moreover, it is seen that at low to moderate pressures, i.e., $p = 0.1$MPa to $p = 1.0$MPa, the facilitating (due to lowering the enthalpy of vaporization) and impeding (due to increasing the heating period) effects of pressure on droplet lifetime tends to balance. Consequently, it results in indiscernible change of droplet lifetime as ambient pressure changes, which is indicated by those results presented to the right side of the vertical dashed line in Fig. 2.

In terms of the droplet lifetime and the unsteadiness factor, we can constitute a theoretical model interpreting the history of droplet surface during the vaporization process. For mathematical convenience, we introduce the normalized droplet diameter and lifetime, defined by

$$d_n = \frac{d}{d_0},\ t_n = \frac{t}{t_{\text{total}}} \tag{64}$$

The droplet size almost remains at the initial instant of the heating stage, i.e.,

$$d_n^2 = 1,\ t_n \ll \Phi_i \tag{65}$$

where the unsteadiness factor Φ_i can be equivalently regarded as the normalized heating time. At the quasi-steady vaporization stage, the droplet surface decays linearly with time, which is consistent with the classic d^2-law, i.e.,

$$d_n^2 = 1 - \frac{1}{1-\Phi_i}(t_n - \Phi_i),\ t_n > \Phi_i \tag{66}$$

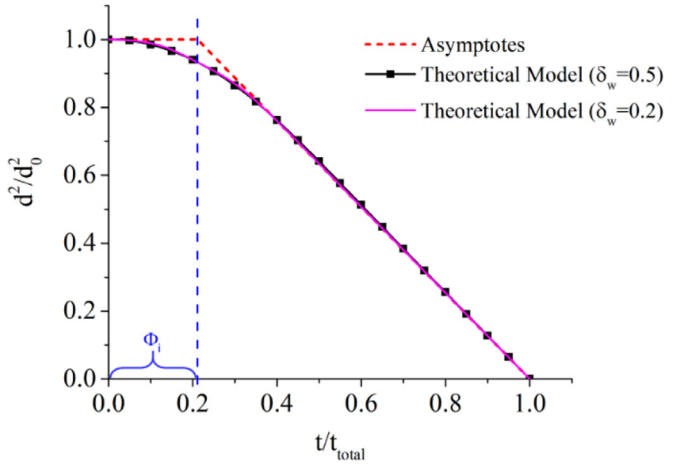

Fig. 3. Schematic of theoretical model for droplet vaporization.

Eqs. (65) and (66) characterize the asymptotic behaviors of the droplet vaporization process. Therefore, an appropriate vaporization model shall satisfy the subsequent conditions, i.e.,

(I) It must spontaneously become Eqs. (65) and (66) respectively at the initial instant of the heating stage and when the droplet undergoes quasi-steady vaporization.

(II) It must experience a smooth transition from Eq. (65) and (66) at some intermediate instant, which depends upon the unsteadiness factor Φ_i.

To constitute the desired vaporization model, capable to interpret the droplet size history during the whole vaporization process, we define a transition function as

$$S(t) = \frac{\tanh\left[\frac{1}{2\delta_w}\left(\frac{t_n}{\Phi_i} - 1\right)\right] + \tanh\frac{1}{2\delta_w}}{\tanh\left[\frac{1}{2\delta_w}\left(\frac{1}{\Phi_i} - 1\right)\right] + \tanh\frac{1}{2\delta_w}} \tag{67}$$

Eq. (67) indicates that $S(t)$ is a normalized function that equals to 0 and 1 at $t_n = 0$ and $t_n = 1$, respectively. The factor δ_w interprets the width of the transition regime such that within an interval, centered at Φ_i with width δ_w, the value of the function $S(t)$ changes from 0.1 to 0.9. Thus, the transition function can characterize the smooth transition from heating stage to quasi-steady vaporization stage. The vaporizations of various fuels at elevated temperatures and pressures share the common feature that the quasi-steady vaporization is preceded by a heating stage during which the droplet size changes slightly. It implies that the transition function can be applied to a variety of fuels.

Using the transition function given by Eq. (67), we constitute the theoretical model for droplet vaporization:

$$\frac{d^2}{d_0^2} = 1 - \frac{S(t)}{1-\Phi_i}[t_n - \Phi_i S(t)] \tag{68}$$

Fig. 3 shows that the present model for droplet vaporization satisfies both requirements (I) and (II), which verifies its mathematical appropriateness and physical plausibility. Moreover, it indicates that the theoretical model is insensitive to the variation of transition function because the predicted droplet size history changes negligibly as the transition width changes from 0.2 to 0.5. Thereby, we shall adopt that $\delta_w = 0.5$ in the subsequent calculation based on the vaporization model.

Fig. 4 compares the droplet size histories predicted by Eq. (68) with experimental results reported by Nomura et al. [6]. For relatively high temperature situations at normal pressure, i.e., $p = 0.1$MPa, the theoretically predicted droplet vaporization rates are slightly greater than those measured in experiments. As shown in Fig. 1, the calculated T_s^0 from the present model tends to be uniformly lower than the wet-bulb temperature at normal pressure condition, which may lead to underestimation of droplet heating time. Meanwhile, due to the same cause, the temperature discrepancy between the droplet surface and the ambience becomes larger, which further facilitates the vaporization process. Thereby, the calculated droplet lifetimes appear to be shorter than those measured in experiments.

It is seen that for droplet vaporizing at high pressures its diameter undergoes discernible increment during the initial heating stage. It can be understood that at elevated pressures, which leads to increasing of droplet surface temperature as well as the average temperature, the thermal expansion effect of the droplet becomes more pronounced. The proportion of heating stage for droplet vaporization at $T = 656$K appears to be discernible larger than the other cases. We hypothesize that at some intermediate instant the droplet diameter increasing due to thermal expansion tends to be in balance with the droplet surface regression caused by vaporization and thereby it yields a prolonged "heating stage" where the droplet size change slightly. As environmental temperature increasing, the vaporization effect starts to dominate over the thermal expansion effect, leading to reduction in the proportion of heating stage, as indicated by droplet vaporization at $T = 746$K.

In this work, we obtained a simplified model for droplet vaporization in which thermal expansion effect was not taken into account. Consequently, discrepancy between the theoretical prediction and experimental results may appear. It merits future study to improve the current theoretical model by considering more factors that have impacts upon the behavior of droplet vaporization, for instance, thermal expansion, the convection in gas phase, and multi-component droplets.

Overall, the theoretically predicted time change of the droplet size during vaporization agrees well with the experimental results both qualitatively and quantitively. The present model can describe the characteristics of droplet vaporization under elevated temperature and pressure conditions, and in particular, the unsteadiness caused by droplet heating can be properly interpreted.

4. Conclusions

We analyze the droplet vaporization problem based on fundamental principles of fluid mechanics and thermodynamics. The transient governing equations are analytically solved after appropriate coordinate transformations. In combination of the matching conditions and the Clausius-Clapeyron relation, the mass fraction of fuel vapor and temperature on the droplet surface can be iteratively determined by Eqs. (43) and (53). Then the characteristic times for droplet heating and vaporization are respectively calculated through Eqs. (48) and (51), whose sum yields the droplet lifetime for vaporization. The theoretically predicted lifetimes agree well with those extrapolated from experiments by Nomura et al. [6]. In terms of unsteadiness factor, defined by Eq. (58), and the transition function, defined by Eq. (67), a theoretical model is constituted, which illustrates the time change of droplet size in the entire vaporization process, given by Eq. (68). It is verified through comparison with the experimental results within wide ranges of temperature (from 450 K to 750 K) and pressure (from 0.1 MPa to 2 MPa). Besides, the theoretical model successfully reveals the conventional recognition that the droplet diameter approximately remains constant at the heating stage, while during the quasi-steady vaporization, the droplet surface shrinks linearly with time according to the d^2-law.

Both experimental observation and the theoretical prediction indicates that the pressure has a dual effect upon droplet lifetime. This is pertinently elucidated based on our theoretical analysis with the help of explicit formula for enthalpy of vaporization, given by Eq. (55). At low to moderate temperatures, the droplet

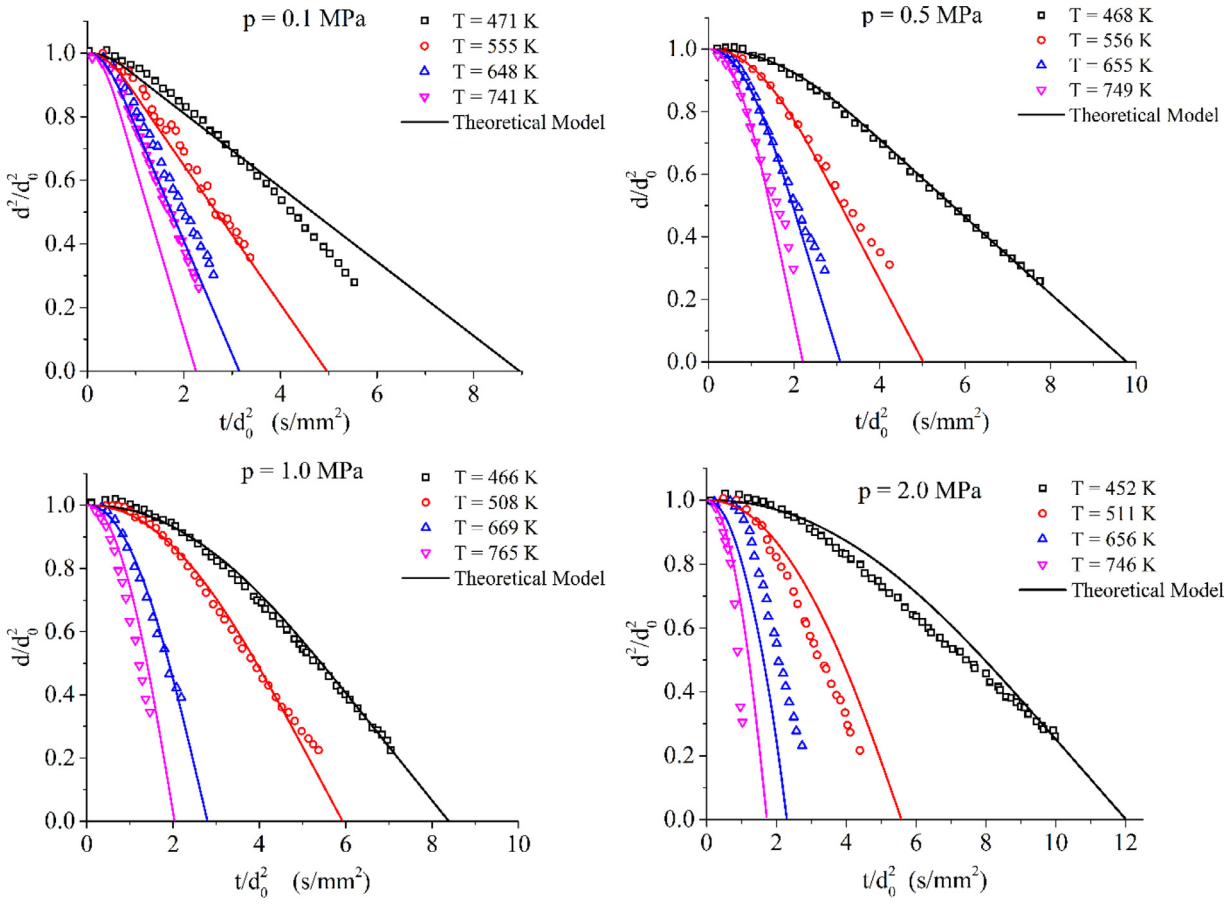

Fig. 4. Comparison between the model prediction and experimental data from Nomura et al. [6]

lifetime increases with pressure due to the reduction of the heat transfer from the hot ambience to the droplet surface. On the other hand, at moderate to high temperatures, increasing the ambient pressure tends to shorten the droplet lifetime. This is because the enthalpy of vaporization decays as the droplet temperature is considerably elevated, which facilitates the vaporization process. At moderate pressures, the facilitating and impeding effects of ambient pressure on droplet lifetime tends to balance, leading to that the droplet lifetime appears to be independent of the ambient pressure.

Declaration of Competing Interest

The authors declare that they have no known competing financial interests or personal relationships that could have appeared to influence the work reported in this paper.

CRediT authorship contribution statement

Dehai Yu: Conceptualization, Methodology, Validation, Writing - original draft. **Zheng Chen:** Conceptualization, Supervision, Writing - review & editing.

Acknowledgement

This work was supported by National Natural Science Foundation of China (nos. 91841302 and 91741126).

Appendix

The thermodynamic and transport properties in both gas and liquid phases are evaluated as follows.

A1. Density

The gas phase is a mixture of fuel (n-heptane) vapor and nitrogen. The mixture density is calculated as

$$\rho_g = Y_{Fs}^0 \rho_{g,F} + \left(1 - Y_{Fs}^0\right)\rho_{g,N} \tag{a1}$$

The densities of fuel vapor ρ_{Fg} and nitrogen ρ_{Ng} are determined by solving the Peng-Robinson equation of state, given by

$$p = \frac{RT}{V_m - b} - \frac{a\left\{1 + f_\omega\left[1 - (T/T_c)^{1/2}\right]\right\}^2}{V_m(V_m + b) + b(V_m - b)} \tag{a2}$$

for pure fuel vapor and nitrogen, respectively. The parameters in Peng-Robinson equation of state are determined by the critical properties and acentric factor ω, i.e.,

$$f_\omega = 0.37464 + 1.54226\omega + 0.26992\omega^2$$

$$a = 0.45724\frac{R^2T_c^2}{p_c}$$

$$b = 0.07780\frac{RT_c}{p_c}$$

Since the pressure considered in this work is considerably less than the critical pressure of either n-heptane or nitrogen, the solubility of nitrogen in the droplet appears to be negligible. Thereby we can consider the droplet could as consisting of pure liquid n-heptane. For situations with $T < T_c$ and $p < p_c$, solving Eq. (a2)

gives three values of molar densities ($1/V_m$), which can be transformed into mass-based densities.

A2. Heat capacity

The heat capacities at constant pressure in gas phase are calculated via the subsequent fitting formulas [46]

$$c_{pg,i} = \frac{a_1}{T_{\rm ch}^2} + \frac{a_2}{T_{\rm ch}} + a_3 + a_4 T_{\rm ch} + a_5 T_{\rm ch}^2 + a_6 T_{\rm ch}^3 + a_7 T_{\rm ch}^4, \quad i = F, \ N \tag{a3}$$

where the characteristic temperature $T_{\rm ch}$ is estimated via the 1/3 rule [36,44] in terms of T_s^0 and T_∞,

$$T_{\rm ch} = \frac{2}{3} T_s^0 + \frac{1}{3} T_\infty \tag{a4}$$

The coefficients a_1 to a_7 for n-heptane and nitrogen are listed as follows

	n-heptane	nitrogen
a_1	-6.1274×10^5	2.2104×10^4
a_2	1.1841×10^4	-3.8185×10^2
a_3	-7.4872×10	6.0827
a_4	2.9185×10^{-1}	-8.5309×10^{-3}
a_5	-3.4168×10^{-4}	1.3846×10^{-5}
a_6	2.1593×10^{-7}	-9.6258×10^{-9}
a_7	-5.6559×10^{-11}	2.5197×10^{-12}

The heat capacity at constant pressure for the gas mixture is estimated by an average weighted by molar fraction of each species, i.e.,

$$c_{pg} = X_{Fs}^0 c_{pg,F} + \left(1 - X_{Fs}^0\right) c_{pg,N} \tag{a5}$$

The molar fraction X_{Fs}^0 is related to the mass fraction Y_{Fs}^0 by

$$X_{Fs}^0 = \frac{Y_{Fs}^0 / W_F}{Y_{Fs}^0 / W_F + \left(1 - Y_{Fs}^0\right)/W_N}$$

The heat capacity of liquid n-heptane is determined by via the following fitting formula, which is derived based on Lee-Kesler equation [47],

$$c_{vl} = a\left(b + c T_s^0\right) \tag{a6}$$

where the coefficients a, b, and c are given by

$$a = 1.4651 + 0.2303 k_w$$
$$b = 0.306469 - 0.16734 s_g$$
$$c = 0.001467 - 0.000551 s_g$$

where k_w is the Watson characterization factor defined by

$$k_w = (1.8 T_{nb})^{1/3} / s_g \tag{a7}$$

where T_{nb} is the normal boiling point of n-heptane and $s_g = \rho_l / \rho_{water}$ is the specific gravity.

A3. Thermal conductivity

The thermal conductivity of n-heptane is calculated through the representative reference equation proposed by Assael et al [48], which is of high accuracy over wide ranges of temperature and pressure.

$$\lambda_{gF}(\rho, T_{\rm ch}) = \lambda_o(T_{\rm ch}) + \Delta\lambda(\rho, T_{\rm ch}) + \Delta\lambda_c(\rho, T_{\rm ch}) \tag{a8}$$

On the right-hand side of Eq. (a8), the first term is the contribution to the thermal conductivity in the dilute-gas limit, while the last term represents the critical enhancement arising from the long-range density fluctuations that occur when the fluid is near its critical point, and the second term denotes the contribution of all other effects to the thermal conductivity of the fluid at elevated pressures.

The mathematical forms for each term are given by

$$\lambda_o(T_r) = \frac{-1.8337 + 16.2572 T_r - 39.0996 T_r^2 + 47.8694 T_r^3 + 15.1925 T_r^4 - 3.3912 T_r^5}{0.2506 - 0.3209 T_r + T_r^2} \tag{a9}$$

where $T_r = T_{\rm ch}/T_c$ is the reduced characteristic temperature.

The residual term is given by

$$\Delta\lambda(\rho, T) = \sum_{i=1}^{5} (B_{1,i} + B_{2,i} T_r)(\rho_r)^i \tag{a10}$$

where the coefficients $B_{1,\,i}$ and $B_{2,\,i}$ are listed as follows

i	$B_{1,i}$ (W m^{-1} K^{-1})	$B_{2,i}$ (W m^{-1} K^{-1})
1	5.17785×10^{-2}	-7.72433×10^{-3}
2	-9.24052×10^{-2}	2.18899×10^{-2}
3	5.11484×10^{-2}	1.71725×10^{-3}
4	-7.76896×10^{-3}	-7.91642×10^{-3}
5	1.21637×10^{-4}	1.83379×10^{-3}

The critical enhancement term is represented by the following empirical expression

$$\Delta\lambda_c(\rho, T) = \frac{C_1}{C_2 + |\Delta T_c|} \exp\left[-C_3 (\Delta\rho_c)^2\right] \tag{a11}$$

where $\Delta T_c = T_{\rm ch}/T_c - 1$ and $\Delta\rho_c = \rho_g/\rho_c - 1$. The coefficients C_1, C_2 and C_3 are estimated by

$$C_1 = 0.7 \times 10^{-3} \text{ W m}^{-1} \text{ K}^{-1}$$
$$C_2 = 7.0 \times 10^{-2}$$
$$C_3 = 1.8 \tag{a12}$$

The thermal conductivity for nitrogen is obtained from the fitting formula [49]

$$\ln \lambda_{gN} = A \ln T_{\rm ch} + \frac{B}{T_{\rm ch}} + \frac{C}{T_{\rm ch}^2} + D \tag{a13}$$

where the coefficients are given by

A	B	C	D
0.85372829	105.18665	−12299.753	0.48299104

The thermal conductivity calculated via Eq. (a13) has unit $10^{-6} \times$ W cm^{-1} K^{-1}.

Similarly, the thermal conductivity of the gas mixture is approximated estimated by

$$\lambda_g = X_{Fs}^0 \lambda_{gF} + \left(1 - X_{Fs}^0\right) \lambda_{gN} \tag{a14}$$

A4. Mass diffusivity

The mass diffusion coefficient is determined based on the Chapman and Enskog's theory, and it is given by a semi-empirical formula [50]

$$D_g = \frac{0.00266 T_{\rm ch}^{3/2}}{p W_{FN}^{1/2} \chi_{FN}^2 \Omega_D} \tag{a15}$$

where W_{FN} is combined molecular weight of fuel and nitrogen, defined by

$$W_{FN} = 2\left(\frac{1}{W_F} + \frac{1}{W_N}\right)^{-1} \tag{a16}$$

and σ_{FN} is the interaction characteristic length defined as the average of characteristic Lennard-Jones lengths of fuel species and nitrogen, i.e.,

$$\chi_{FN} = \frac{1}{2}(\sigma_F + \sigma_N) \tag{a17}$$

The σ_F and σ_N can be determined in terms of critical densities ρ_c of the fuel species and nitrogen, respectively. The dimensionless collision integral Ω_D can be calculated from the following empirical formula

$$\Omega_D = \frac{A}{T^{*B}} + \frac{C}{\exp(DT^*)} + \frac{E}{\exp(FT^*)} + \frac{G}{\exp(HT^*)} \tag{a18}$$

The T^* is a dimensionless temperature defined by $T^* = kT_{\mathrm{ch}}/\sqrt{\varepsilon_F \varepsilon_N}$, where ε_F and ε_N are characteristic Lennard-Jones energies of fuel species and nitrogen, respectively. The coefficients A to G are given as follows

A	B	C	D	E	F	G	H
1.06036	0.15610	0.19300	0.47635	1.03587	1.52996	1.76474	3.89411

References

[1] W.A. Sirignano, Fuel droplet vaporization and spray combustion theory, Prog. Energ. Combust. 9 (4) (1983) 291–322.
[2] W. Han, Z. Chen, Effects of finite-rate droplet evaporation on the ignition and propagation of premixed spherical spray flame, Combust. Flame 162 (5) (2015) 2128–2139.
[3] A.H. Lefebvre, V.G. McDonell, Atomization and Sprays, CRC Press, 2017.
[4] H. Jia, G. Gogos, Investigation of liquid droplet evaporation in subcritical and supercritical gaseous environments, J. Thermophys. Heat Transf. 6 (4) (1992) 738–745.
[5] J.P. Hartfield, P. Farrell, Droplet vaporization in a high-pressure gas, J. Heat Transf. 115 (1993) 699–706.
[6] H. Nomura, Y. Ujiie, H.J. Rath, J.i. Sato, M. Kono, Experimental study on high--pressure droplet evaporation using microgravity conditions, in: Symposium (International) on Combustion, 1996, pp. 1267–1273.
[7] R. Matlosz, S. Leipziger, T. Torda, Investigation of liquid drop evaporation in a high temperature and high pressure environment, Int. J. Heat Mass Transf. 15 (4) (1972) 831–852.
[8] K. Hsieh, J. Shuen, V. Yang, Droplet vaporization in high-pressure environments I: near critical conditions, Combust. Sci. Technol. 76 (1–3) (1991) 111–132.
[9] H. Zhang, V. Raghavan, G. Gogos, Subcritical and supercritical droplet evaporation within a zero-gravity environment: low Weber number relative motion, Int. Commun. Heat Mass 35 (4) (2008) 385–394.
[10] G.C. Hsiao, H. Meng, V. Yang, Pressure-coupled vaporization response of n-pentane fuel droplet at subcritical and supercritical conditions, Proc. Combust. Inst. 33 (2) (2011) 1997–2003.
[11] S. Ray, V. Raghavan, G. Gogos, Two-phase transient simulations of evaporation characteristics of two-component liquid fuel droplets at high pressures, Int. J. Multiph. Flow 111 (2019) 294–309.
[12] D.E. Rosner, W. Chang, Transient evaporation and combustion of a fuel droplet near its critical temperature, Combust. Sci. Technol. 7 (4) (1973) 145–158.
[13] M. Arias-Zugasti, P.L. Garcia-Ybarra, J.L. Castillo, Unsteady effects in droplet vaporization lifetimes at subcritical and supercritical conditions, Combust. Sci. Technol. 153 (1) (2000) 179–191.
[14] G. Zhu, S. Aggarwal, Transient supercritical droplet evaporation with emphasis on the effects of equation of state, Int. J. Heat Mass Transf. 43 (7) (2000) 1157–1171.
[15] S. Sazhin, W. Abdelghaffar, E. Sazhina, M. Heikal, Models for droplet transient heating: effects on droplet evaporation, ignition, and break-up, Int. J. Therm. Sci. 44 (7) (2005) 610–622.
[16] A. Arabkhalaj, A. Azimi, H. Ghassemi, R.S. Markadeh, A fully transient approach on evaporation of multi-component droplets, Appl. Therm. Eng. 125 (2017) 584–595.
[17] A. Azimi, A. Arabkhalaj, H. Ghassemi, R.S. Markadeh, Effect of unsteadiness on droplet evaporation, Int. J. Therm. Sci. 120 (2017) 354–365.
[18] J. Shuen, V. Yang, C. Hsiao, Combustion of liquid-fuel droplets in supercritical conditions, Combust. Flame 89 (3-4) (1992) 299–319.
[19] H. Jia, G. Gogos, Droplet vaporization in subcritical and supercritical environments; high vs low pressure modelling, Acta Astronaut. 32 (2) (1994) 121–129.
[20] G. Strotos, M. Gavaises, A. Theodorakakos, G. Bergeles, Numerical investigation of the evaporation of two-component droplets, Fuel 90 (4) (2011) 1492–1507.
[21] G. Strotos, I. Malgarinos, N. Nikolopoulos, M. Gavaises, Predicting the evaporation rate of stationary droplets with the VOF methodology for a wide range of ambient temperature conditions, Int. J. Therm. Sci. 109 (2016) 253–262.
[22] C.K. Law, Combustion Physics, Cambridge University Press, 2010.
[23] H. Meng, G. Hsiao, V. Yang, J. Shuen, Transport and dynamics of liquid oxygen droplets in supercritical hydrogen streams, J. Fluid Mech. 527 (2005) 115–139.
[24] M. Renksizbulut, R. Haywood, Transient droplet evaporation with variable properties and internal circulation at intermediate Reynolds numbers, Int. J. Multiph. Flow 14 (2) (1988) 189–202.
[25] A. Williams, Combustion of Liquid Fuel Sprays, Butterworth-Heinemann, 2013.
[26] A. Crespo, A. Linan, Unsteady effects in droplet evaporation and combustion, Combust. Sci. Technol. 11 (1-2) (1975) 9–18.
[27] Y. Wu, X. Zhang, X. Zhang, Simplified analysis of heat and mass transfer model in droplet evaporation process, Appl. Therm. Eng. 99 (2016) 938–943.
[28] C.K. Law, Unsteady droplet combustion with droplet heating, Combust. Flame 26 (1976) 17–22.
[29] C.K. Law, W. Sirignano, Unsteady droplet combustion with droplet heating—II: conduction limit, Combust. Flame 28 (1977) 175–186.
[30] W. Sirignano, C. Law, Transient heating and liquid-phase mass diffusion in fuel droplet vaporization, in: Evaporation—Combustion of Fuels, ACS Publications, 1978, pp. 3–26.
[31] C.K. Law, Recent advances in droplet vaporization and combustion, Prog. Energy Combust. Sci. 8 (3) (1982) 171–201.
[32] P. Botros, C. Law, W. Sirignano, Droplet combustion in a reactive environment, Combust. Sci. Technol. 21 (3-4) (1980) 123–130.
[33] M. Shusser, The influence of thermal expansion flow on droplet evaporation, Int. J. Multiph. Flow 33 (1) (2007) 40–50.
[34] S. Tonini, G. Cossali, An analytical model of liquid drop evaporation in gaseous environment, Int. J. Therm. Sci. 57 (2012) 45–53.
[35] G. Cossali, S. Tonini, An analytical model of heat and mass transfer from liquid drops with temperature dependence of gas thermo-physical properties, Int. J. Heat Mass Transf. 138 (2019) 1166–1177.
[36] A.Y. Snegirev, Transient temperature gradient in a single-component vaporizing droplet, Int. J. Heat Mass Transf. 65 (2013) 80–94.
[37] S. Sazhin, I. Gusev, P. Krutitskii, M. Heikal, Transient heating of a semitransparent spherical body immersed into a gas with inhomogeneous temperature distribution, Int. J. Therm. Sci. 50 (7) (2011) 1215–1222.
[38] S.S. Sazhin, P.A. Krutitskii, S.B. Martynov, D. Mason, M.R. Heikal, E.M. Sazhina, Transient heating of a semitransparent spherical body, Int. J. Therm. Sci. 46 (5) (2007) 444–457.
[39] S. Sazhin, P. Krutitskii, W. Abdelghaffar, E. Sazhina, S. Mikhalovsky, S. Meikle, M. Heikal, Transient heating of diesel fuel droplets, Int. J. Heat Mass Transf. 47 (14-16) (2004) 3327–3340.
[40] B.E. Poling, J.M. Prausnitz, J.P. O'connell, The Properties of Gases and Liquids, fifth ed., Mcgraw-Hill, New York, 2001.
[41] D. Yu, Z. Chen, A theoretical analysis on enthalpy of vaporization: temperature-dependence and singularity at the critical state, Fluid Ph. Equilibria (2020) 112611.
[42] M. Campostrini, A. Pelissetto, P. Rossi, E. Vicari, 25th-order high-temperature expansion results for three-dimensional Ising-like systems on the simple-cubic lattice, Phys. Rev. E 65 (6) (2002) 066127.
[43] J. Cahoon, The first coordination number for liquid metals, Can. J. Phys. 82 (4) (2004) 291–301.
[44] R. Miller, K. Harstad, J. Bellan, Evaluation of equilibrium and non-equilibrium evaporation models for many-droplet gas-liquid flow simulations, Int. J. Multiph. Flow 24 (6) (1998) 1025–1055.
[45] M. Yuen, L. Chen, On drag of evaporating liquid droplets, Combust. Sci. Technol. 14 (1976) 147–154.
[46] B.J. McBride, NASA Glenn Coefficients for Calculating Thermodynamic Properties of Individual Species, National Aeronautics and Space Administration, John H. Glenn Research Center, 2002.
[47] M. Riazi, Characterization and Properties of Petroleum Fractions, ASTM International, 2005.
[48] M.J. Assael, I. Bogdanou, S.K. Mylona, M.L. Huber, R.A. Perkins, V. Vesovic, Reference correlation of the thermal conductivity of n-heptane from the triple point to 600 K and up to 250 MPa, J. Phys. Chem. Ref. 42 (2) (2013) 023101.
[49] R.A. Svehla, Transport coefficients for the NASA Lewis chemical equilibrium program, (1995).
[50] K.K. Kuo, Principles of Combustion, John Wiley & Sons, Inc., 2005.